ACTA UNIVERSITATIS AGRICULTURAE ET SILVICULTURAE MENDELIANAE BRUNENSIS
SBORNÍK MENDELOVY UNIVERZITY V BRNĚ

Volume LVIII 1 Number 1, 2010

NEW ALGORITHM FOR BIOLOGICAL OBJECTS' SHAPE EVALUATION AND DATA REDUCTION

S. Bartoň, L. Severa, J. Buchar

Received: September 2, 2009

Abstract

BARTOŇ, S., SEVERA, L. BUCHAR, J.: *New algorithm for biological objects' shape evaluation and data reduction.* Acta univ. agric. et silvic. Mendel. Brun., 2010, LVIII, No. 1, pp. 13–20

The paper presents the software procedure (using MAPLE 11) intended for considerable reduction of digital image data set to more easily treatable extent. The example with image of peach stone is presented. Peach stone, displayed on the digital photo, was represented as a polygon described by the coordinates of the pixels creating its perimeter. The photos taken in high resolution (and corresponding data sets) contain coordinates of thousands of pixels – polygon's vertexes. Presented approach substitutes this polygon by the new one, where smaller number of vertexes is used. The task is solved by use of adapted least squares method. The presented algorithm enables reduction of number of vertexes to 10% of its original extent with acceptable accuracy +/– one pixel (distance between initial and final polygon). The procedure can be used for processing of similar types of 2D images and acceleration of following computations.

image processing, data reduction, least square method

The acquisition and analysis of the visual information represents powerful tool for interpretation of large range of input data. The origin of computer vision is intimately intertwined with computer history, having been motivated by a wide spectrum of important applications such as robotics, biology, medicine, industry and physics, but also agricultural and food sciences in last decades. Among all different aspects underlying visual information, the shape of the objects certainly plays a special role. The multidisciplinarity of image analysis, with respect to both techniques and applications, has motivated a rich and impressive set of information resources represented e.g. by book Costa and Cesar (2009).

Precise and correct image processing enables solving problems of multidisciplinary nature, completing images and objects in terms of features (implying several distinct objects to be mapped into the same representation), pattern recognition used for segmenting an image into its constituent parts, proper validation of algorithms, and/or improving the relation between continuous and discrete approaches.

In fact "computer vision" (or generally image processing) often requires, sometimes real time, processing of a very large and heterogeneous data sets (including shape, spatial orientation, color, texture, motion, etc.). Extensive image files or series of images are processed e.g. in medicine (Söhn et al., 2005; Zagrodsky et al., 2005; Li et al., 2006), biological studies (Tománková et al., 2006; Klotz et al., 2007), but also in agricultural sciences (Yahya et al., 2009; Zadravec and Žalik, 2009; Zhong et al., 2009) or food sciences (Havlíček et al., 2008; Severa, 2007; Severa, 2008). In spite of increasing hardware performance, large or sometimes huge data sets often cause problems and certain data reduction, regularization and/or modification is needed. There are several generally accepted approaches to achieve this task. One of the most commonly used methods is Principal Component Analysis (PCA). Principal Component Analysis is a technique that simplifies data sets by reducing their dimensionality. It is often used to decompose shape variability into a reduced set of interpretable components. It is an orthogonal linear transformation that spans a subspace, which approximates the data optimally in a least-squares sense (Jolliffe, 1986). This is accomplished by maximizing the variance of the transformed coordinates. If the dimensionality of the data is to be reduced to N, an equivalent formulation of PCA is to find the N-set of orthonormal vectors, grouped in the P matrix, which minimizes the error made when

reconstructing the original data points in the data set. This method was successfully used in number of works – see e.g. Vidal et al. (2005), Iglesias et al. (2007), Havlíček et al. (2008). There are alternative approaches such as LDA (Linear Discriminant Analysis) – see e.g. Wang et al. (2004) or PFA (Principal Factor Analysis) – see e.g. Ballester et al. (2005).

This paper presents completely different approach, where input image data are significantly reduced (to 10% of original extent) by means of MAPLE 11 algorithm without loss of precision. Example with peach stone is presented. Reduced data sets can be consequently used for faster processing and/or further utilization. MAPLE software environment have been successfully used for determination of agricultural products shape (Bartoň, 2000; Bartoň, 2007; Bartoň, 2008).

MATERIAL AND METHODS

Digital photo

A sample digital photo of peach stone of *Red Heaven* variety (harvested in July 2008 in region of Southern Moravia) has been used. But any similar object of natural of artificial origin could have been used. The photo has been taken by digital camera Olympus SP–55OUZ with resolution of 7.1 Mpixels, see Fig. 1.

Processing software

A software MAPLE 11, classic has been used to perform all presented calculations.

Computing procedure

The best line

Let us assume polygon given by the list of N points with coordinates $[[X_1, Y_1], \ldots, [X_i, Y_i], \ldots, [X_N, Y_N]]$. Let us select sublist of vertexes $N_1 \ldots N_2$, $1 <= N_1 < N_2 <= N$, $N_2 - N_1 >= 2$. The task is to find parameters of common line p_1 which will minimize $\sum_{i=N1}^{N2} d_i^2$, where d_i = length of the line segment between i_{th} and $p_{i_{th}}$ point. The point is the intersection of the line perpendicular to the line *p1* going through i_{th} point with the line *p1*.

Lists of lines and corresponding points

After definition of best line, the procedure can continue in computing of best line for remaining points from the list of the vertexes and smoothing the polygon.

Estimating of accuracy

After polygon approximation it is possible to compute distances d_i for input polygon vertexes using corresponding line segments. It is possible to compute their average values and variance. These values may be used to determine accuracy of approximation.

Maple procedure

The complete Maple procedure for presented approach can be seen in the first author's personal web pages: *user.mendelu.cz/barton*.

RESULTS AND DISCUSSION

The best line

The best form of the line *p1*, corresponding to the above mentioned problem is $p1 := (x - Qx)\sin(\phi) + (Qy - y)\cos(\phi) = 0$, where $[Qx, Qy]$ are coordinates of the point lying on this line and ϕ is its direction angle, see Fig. 2.

In this case the coordinates of the $p_{i_{th}}$ point are as follows:

$$Xp_i = (-Qx\cos(\phi) - \sin(\phi)\,Qy + \sin(\phi)\,Y_i + X_i\cos(\phi))\cos(\phi) + Qx$$

and

$$Yp_i = (-Qx\cos(\phi) - \sin(\phi)\,Qy + \sin(\phi)\,Y_i + X_i\cos(\phi))\sin(\phi) + Qy. \quad (1)$$

1: *A sample digital photo of the peach stone*

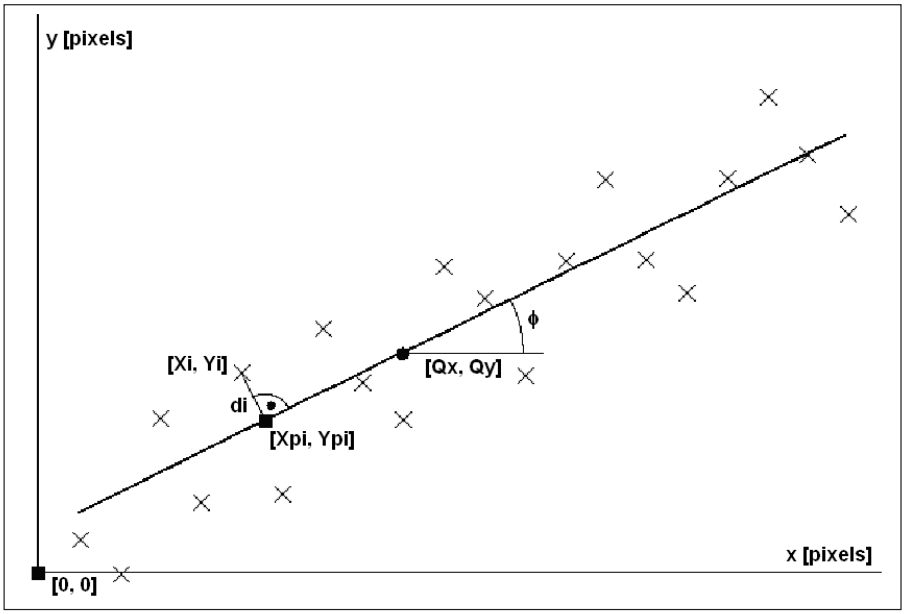

2: *The best line*

The square of the distance from the line *p1* is $d_i^2 = (X_i - Xp_i)^2 + (Y_i - Yp_i)^2$, where Xp_i and Yp_i are defined by the equation (1). The sum of the squares of the distances d_i for all N points is $\sum_{i=N1}^{N2} d_i^2 = SoS$,

$$SoS = -2\cos(\phi)\sin(\phi)(QyQx(N2 - N1 + 1) + \Sigma 2 - Qy\,\Sigma 3 - Qy\,\Sigma 4) + ((N2 - N1 + 1)\,Qx^2 - 2Qx\,\Sigma_3 + \Sigma_1)\sin(\phi)^2 + ((N2 - N1 + 1)\,Qy^2 - 2Qy\,\Sigma_4 + \Sigma_5)\cos(\phi)^2, \quad (2)$$

where

$$\Sigma_1 = \sum_{i=N1}^{N2} X_i^2,\ \Sigma_2 = \sum_{i=N1}^{N2} Y_i X_i,\ \Sigma_3 = \sum_{i=N1}^{N2} X_i,\ \Sigma_4 = \sum_{i=N1}^{N2} Y_i,\ \Sigma_5 = \sum_{i=N1}^{N2} Y_i^2.$$

These substitutions accelerate computation of $\sum_{i=N1}^{N2} d_i^2$, because it is faster to calculate all sums only ones and to substitute obtained results instead of computing each sum as indicated in (2) or in the following expressions. The condition for the global minimum of $SoS(Qx, Qy, \phi)$ is $\frac{\partial}{\partial Qx} SoS = 0$, $\frac{\partial}{\partial Qy} SoS = 0$ and $\frac{\partial}{\partial Q\phi} SoS = 0$. First and second equation consequently yields in $Qx = \frac{\Sigma_3}{N2 - N1 + 1}$, $Qy = \frac{\Sigma_4}{N2 - N1 + 1}$. If these values are substituted into the third equation, the result has a following form:

$$S_2 \sin(\phi)^2 + S_1 \cos(\phi)\sin(\phi) + S_3 \cos(\phi)^2 = 0,$$

where below listed substitutions (3)

$$S_1 = 2\Sigma_4^2 - 2\Sigma_1 N_1 + 2\Sigma_1 - 2\Sigma_5 - 2\Sigma_5 N_2 + 2\Sigma_5 N_1 - 2\Sigma_3^2 + 2\Sigma_1 N_2,$$

$$S_2 = -2\Sigma_4\Sigma_3 + 2\Sigma_2 N_2 - 2\Sigma_2 N_1 + 2\Sigma_2,$$

$$S_3 = 2\Sigma_2 N_1 - 2\Sigma_2 - 2\Sigma_2 N_2 + 2\Sigma_4\Sigma_3$$

simplify equation (3) and its solution for ϕ. Equation (3) has two roots:

$$\phi_1 = \arctan\left(-\frac{S_1}{2} + \frac{\sqrt{S_1^2 - 4S_2S_3}}{2S_2}\right) \text{ and}$$

$$\phi_2 = \arctan\left(\frac{S_1}{2} + \frac{\sqrt{S_1^2 - 4S_2S_3}}{2S_2}\right). \quad (4)$$

The first root leads to the global minimum of the *SoS*, the second one to the global maximum. Therefore it is possible to continue with $\phi = \phi_1$. Following substitution

$$\cos(\phi) = \frac{S_2}{\sqrt{2S_2^2 + S_1 2 + S_1\sqrt{S_1 2 - 4S_2S_3} - 2S_2S_3}} \text{ and}$$

$$\sin(\phi) = \frac{(S_1 + \sqrt{S_1^2 - 4S_2S_3})\sqrt{2}}{\sqrt{2S_2^2 + S_1 2 + S_1\sqrt{S_1 2 - 4S_2S_3} - 2S_2S_3 2}} \quad (5)$$

will simplify computations of (4). In special cases, when line *p1* is parallel with *x* or *y* axis $S_2 = 0$, this substitution converts into $\cos(\phi) = 0$, $\sin(\phi) = 1$ or $\cos(\phi) = 0$, $\sin(\phi) = 0$. In these cases, proper values of $\cos(\phi)$ and $\sin(\phi)$ must be found, to obtain smaller value of *SoS*.

Lists of lines and corresponding points

The best line for the first three points from the list of vertexes can be computed as follows. Let us assume *N1=1* and *N2=3* for this particular case. The best line *p1* can be found for each point with consequent computing of corresponding square of the distance d_i and finding the maximum of distances $Dist = max([d_{N1}, \ldots, d_i, \ldots, d_{N2}]$. If the value is smaller than predefined accuracy *L*, it is possible to increase *N2=N2+1* and repeat the whole process until accuracy is satisfying. Values of *N2*, correspond-

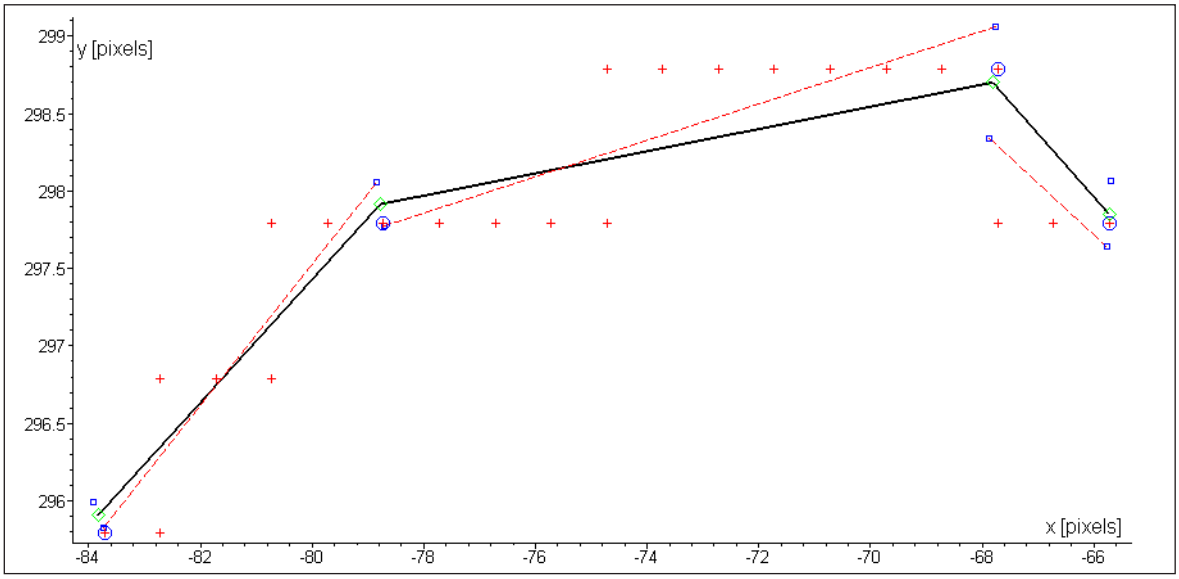

3: *The best line segments and part of corresponding polygon*

ing values of *Qx, Qy, cos(ϕ), sin(ϕ)* describing the best line for the vertexes N1 … N2, and *Dist* can be stored into the lists. The highest *N2* satisfying condition *Dist* < *kL* can be determined from these lists, where *k* is the correction value depending on smoothness of the polygon. If the polygon is smooth $k \to 0.5$, for non-smooth polygons $k \to 0.2$. It is possible to use the value of $k \sim 0.5$, but it must be considered that value *Dist* is function of *N2* and if it ones exceeds *k L*, it may be again lower for higher value of *N2*. This approach leads to higher number of final polygon vertexes. In this case the data reduction will not be so effective. The reason, why the value $k = 1$ cannot be used will be discussed later.

As a next step, the points $[X_{p_{N1}}, Y_{p_{N1}}]$, $[X_{p_{N2}}, Y_{p_{N2}}]$ must be recorded into the list *LXY*, ordinary numbers of the border points *N2* are recorded into list *LN2*, and value *N1* put equal to *N2*, (*N1* = *N2*). The whole process can be repeated with the subsequent vertexes from the list of polygon vertexes. The procedure is repeated until *N2* < *N*. Finally, the both lists will contain *n* elements. The list *LXY* can be displayed as a list of separate line segments approximating initial polygon. The ordinary numbers of vertexes of the input polygon corresponding to the *i-th* line can be picked from the list *LN2* as series if integer numbers from $LN2_{2i-1}$ to $LN2_{2i}$. These lists contain information about line segment – best line and input polygon vertexes corresponding to the line segment. But the line segments are not connected one with each other – see Fig. 3. The best line segments are displayed as a red-dashed line, input polygon vertexes are displayed as red crosses and polygon vertexes with ordinary numbers *N2* are blue-circled. These points correspond to endpoints of the best line segments.

The endpoint of one line segment $[X_{p_{N2}}, Y_{p_{N2}}]$ and initial point of the subsequent line segment $[X_{p_{N1}}, Y_{p_{N1}}]$ correspond to the same vertex of the input polygon. These points are very close, but not identical, because they correspond to the different line segments. The points are displayed in Fig. 3 as blue boxes – end points of the best line segments. These couples of points can be substituted by their midpoints and they are displayed as green diamonds $[X_c, Y_c] = 5([X_{p_{N2}}, Y_{p_{N2}}] + [X_{p_{N1}}, Y_{p_{N1}}]$ in Fig. 3. As a result, continuous curve is obtained, displayed as black line segments, creating polygon with reduced number of vertexes approximating input polygon. Center points will be recorded in a new list *LC*. Because new polygon vertex $[X_c, Y_c]$ is a midpoint corresponding to the projection of the same vertex of the initial polygon to different best lines, this point does not lay on these best lines, but it is close to both of them and the new line segments do not correspond to the preceding line segments – best lines. Therefore it is necessary to put $k<1$. As $k \to 0$, these line segments are shorter, the number of vertexes of the final polygon increases, but accuracy of the approximation is better. Different scale for *x* and *y* axis is used for better overview of Fig. 3. Thus expected right angles are displayed as distorted.

The result can be displayed graphically, see Fig. 4. The figure displays peach stone perimeter described by 3866 red points. Corresponding polygon is substituted by polygon with 109 vertexes with predefined accuracy of 5 pixels. Approximating polygon is displayed by blue line and its vertexes are indicated by blue circles. Since the difference between blue and red line is smaller then line thickness itself, the blue line is not visible. It can be seen that with data reduction *1:35*, the accuracy is satisfying.

Estimating of the accuracy

The most effective method is to compute absolute value d_i and argument ϕ_i of the vector $v_i = [X_i - X_{p_i}, Y_i - Y_{p_i}]$, see Fig. 2, which can be used for the demonstration of accuracy precision. If the best line seg-

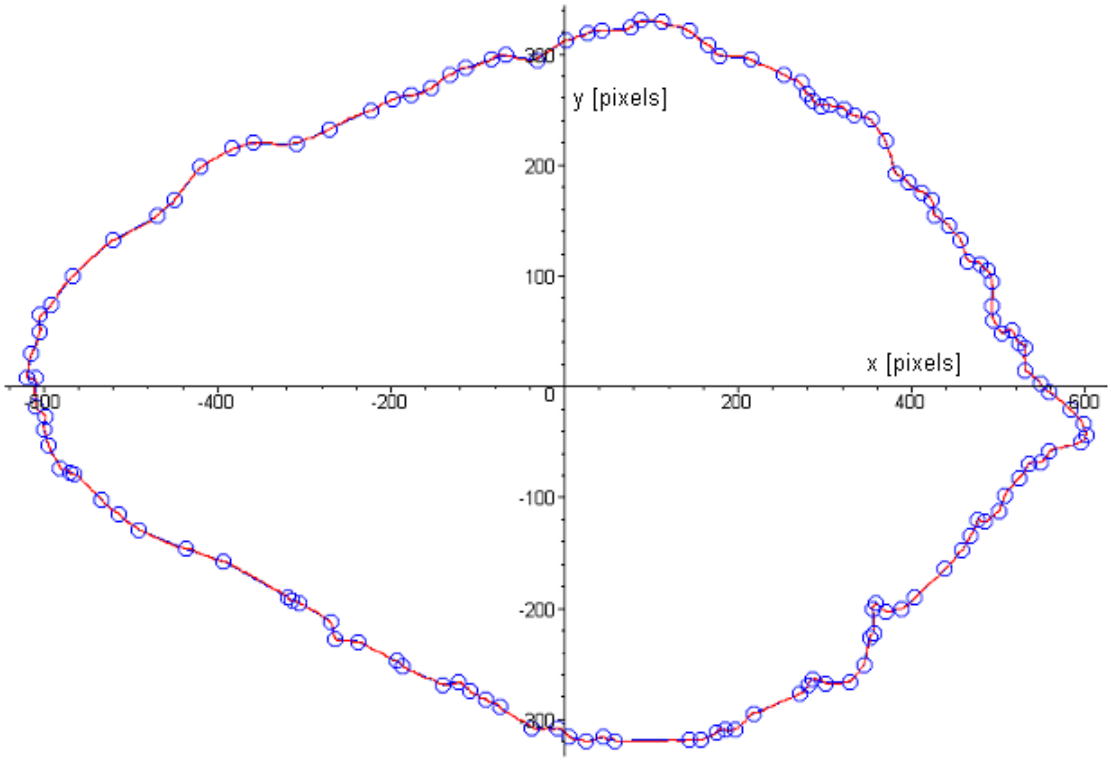

4: *Peach stone shape and its approximation*

ment is defined by its endpoints, $[X_{c1}, Y_{c1}]$ and $[X_{c2}, Y_{c2}]$, see previous section, the distance d_i and orientation ϕ_i can be computed using very simple expressions:

$$d_i = \frac{(X_{c2} - X_{c1})\, Y_i - (Y_{c2} - Y_{c1})\, X_i + X_{c1} Y_{c2} - X_{c2} Y_{c1}}{\sqrt{(X_{c2}{}^2 - X_{c1})^2 + (Y_{c2} - Y_{c1})^2}},$$

$$\phi_i = \arctan\left(\frac{Y_{c1} - Y_{c2}}{X_{c2} - X_{c1}}\right),$$

where (6)

$$X_{c2} = LC_{2j-1,1},\ Y_{c2} = LC_{2j-1,2},\ X_{c1} = LC_{2j,1},\ Y_{c1} = LC_{2j,2},$$

$$LN2_j <= i <= LN2_{j+1} \text{ and } 1 <= j <= n.$$

This approach enables to display accuracy in polar coordinates. For the peach stone presented in Fig. 4, the corresponding accuracy is visualized in Fig. 5. As can be seen, the real accuracy is +/– 2 pixels only. It means that the worst accuracy achieved is about 0.3 % of the object size and the average accuracy indicated by the thick blue line is +/– 0.7 pixels, approximately 0.1%. Variances of the accuracy are displayed as the thin blue lines.

It is possible to plot vertexes of the input polygon and the resulting polygon. The example with distances d_i magnified 25-times is shown in Fig. 6.

It is possible to complete the algorithm by weight list – significance of individual points, *W*. The weight list is intended pro data processing in the softwares directly computing optimum regression function. The relations can be determined as a mean of length value of both segments trajecting through the points. The relation has a following form:

$$W_i = \frac{\sqrt{(X_{c_{i-1}} - X_{c_i})^2 + (Y_{c_{i-1}} - Y_{c_i})^2} + \sqrt{(X_{c_{i+1}} - X_{c_i})^2 + (Y_{c_{i+1}} - Y_{c_i})}}{2}. \quad (7)$$

The difference between regression function with and/or without including of weights is displayed in Fig. 7. The red line represents the function approximating the stone's shape in polar coordinates with coordinate origin in *[129.58, 46.647]*,

$$\begin{aligned} Red = {} & 388.90 - 92.140\cos(f) - 56.561\sin(f) + \\ & 102.11\cos(2.f) \\ & + 2.1903\sin(2.f) - 37.708\cos(3.f) - 15.099\sin(3.f) \\ & + 48.019\cos(4.f) - 0.045109\sin(4.f) - 20.729\cos(5.f) \\ & - 12.624\sin(5.f) + 17.420\cos(6.f) - 3.9376\sin(6.f) \\ & - 9.1169\cos(7.f) - 9.8685\sin(7.f) + 8.3158\cos(8.f) \\ & - 2.7700\sin(8.f) - 9.0515\cos(9.f) - 6.4355\sin(9.f) \end{aligned} \quad (8)$$

The blue line represents the regression function including weights. The coordinates origin is situated in *[1.071, 50.786]*.

$$\begin{aligned} Blue = {} & 394.34 + 6.5714\cos(f) - 61.163\sin(f) + 109.42\cos(2.f) \\ & - 4.0914\sin(2.f) - 27.195\cos(3.f) - 17.868\sin(3.f) \\ & + 39.961\cos(4.f) - 0.44939\sin(4.f) - 8.1234\cos(5.f) \\ & - 11.572\sin(5.f) + 17.217\cos(6.f) - 1.2986\sin(6.f) \\ & - 4.8608\cos(7.f) - 8.3769\sin(7.f) + 4.5218\cos(8.f) \\ & - 2.7134\sin(8.f) - 0.051671\cos(9.f) - 9.8102\sin(9.f) \end{aligned} \quad (9)$$

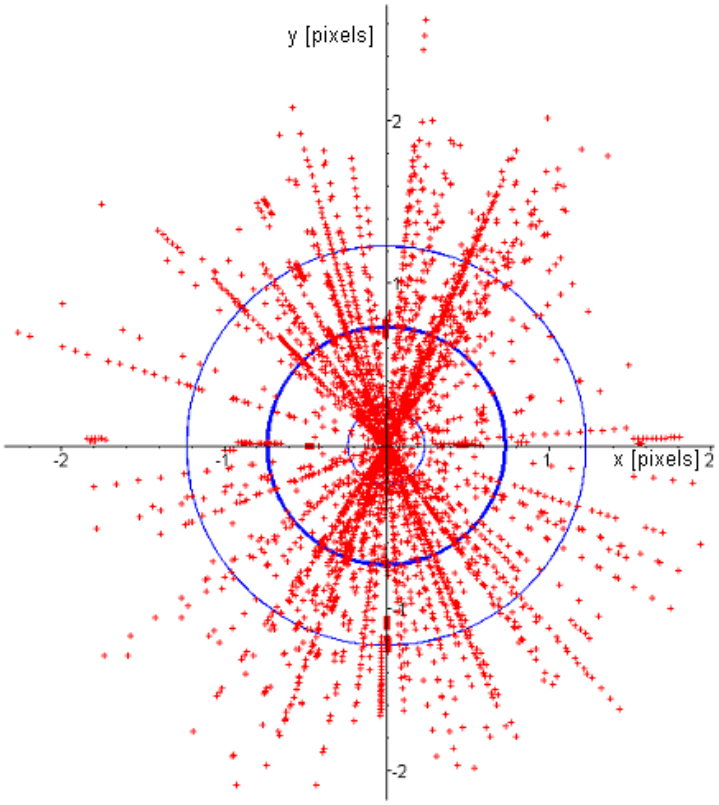

5: *Visualisation of accuracy approximation*

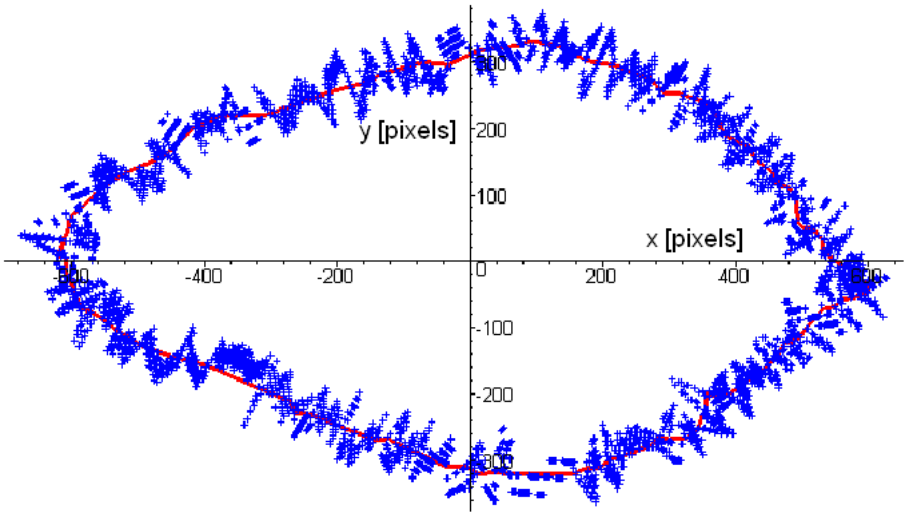

6: *The distance between input and resulting polygons (d_i magnified 25x)*

SUMMARY

Extensive image files or series of images are to be often processed and such procedures can represent demanding task for hardware as well as software environment. Partial data reduction with maintaining the original information and achievement of maximum accuracy is thus effective and useful tool for further computations or generally image data processing. This paper introduces the software approach of reducing the large volume of digital image data to 3 % of its original extent. MAPLE 11 classic was used to perform all presented computations. Digital image (resolution of 7.1 Mpixels) of peach stone was used as an input file. Object displayed on the digital photo, was represented by a polygon. This polygon was described by the pixels' coordinates, where individual pixels created the object's

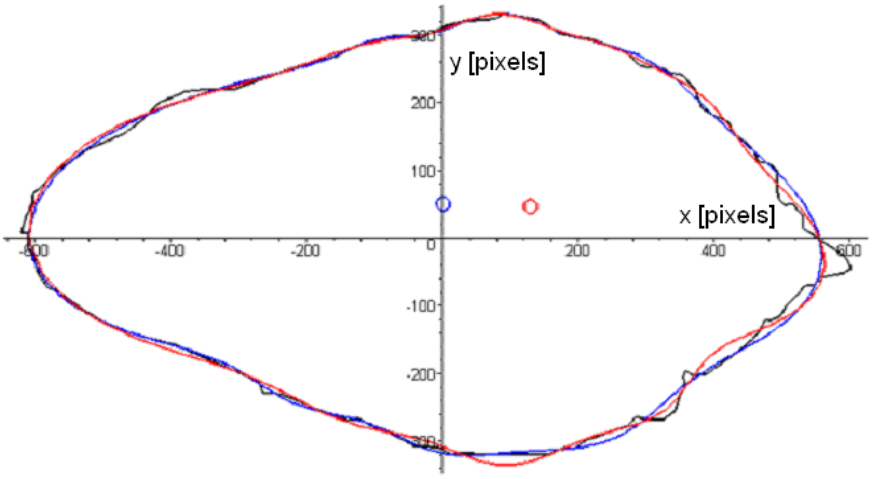

7: *Regression function with/without weights included, blue and red line respectively*

perimeter. In the given example, the object's perimeter consisted of 3866 pixels (polygon's vertexes). Given polygon was substituted by the new one with 109 vertexes. The list of vertexes of the input polygon must be sorted in such way, that line segments connecting consecutive points create perimeter of the polygon. Vertexes must be therefore sorted clockwise or counterclockwise. Average displacement between approximating and input polygon was +/– 0.7 pixels (which represents 0.1% of the object size) with maximum displacement approximately 2 pixels (0.3 % of the object size).
Proposed procedure is of general nature and can be used for data reduction in case of other biological as well as artificial shapes. It can serve as an effective and precise tool for acceleration of processing computing and for enabling the calculation itself on less powerful hardware, such as common PC with MS EXCEL and/or in case of data processing using non-linear regression methods.

SOUHRN

Nový algoritmus pro stanovení tvaru biologických objektů s redukcí dat

Zpracování digitálních obrazů klade velmi vysoké požadavky na technické i programové vybavení počítače. Proto se jeví redukce objemu zpracovávaných dat při zachování maximální možné přesnosti jako významný nástroj, použitelný zejména v oblasti zpracovávání digitálních obrazových informací.
V předkládaném článku je popsán postup redukce objemu zpracovávaných dat na 3 % původní velikosti. Pro vypracování algoritmu byl použit program Maple 11 classic. Jako vstupní obraz byl použit obrys broskvové pecky, sejmutý v rozlišení 7.1 Mpixelu. Obrys je zaznamenán v souboru jako polygon, popsaný pomocí souřadnic jednotlivých vrcholů tak, že úsečka spojující po sobě následující vrcholy tvoří obvod polygonu. Proto vrcholy vstupního polygonu musí být v seznamu uspořádány ve směru nebo proti směru pohybu hodinových ručiček. V použitém případě je obrys tvořen polygonem o 3866 vrcholech a byl nahrazen polygonem o 109 vrcholech. Průměrný rozdíl vzdáleností mezi originálním a aproximujícím polygonem činí +/–0.7 pixelu, což činí 0,1% velikosti objektu a nejvyšší vzdálenost je přibližně dva pixely, což je 0,3% velikosti objektu.
Předkládaný algoritmus je zcela obecný a může být použit pro redukci objemu dat popisujících i jiné biologické nebo další objekty. Může sloužit jako výkonný a přesný nástroj vhodný ke zrychleni zpracování obrazu a může umožnit zpracování obrazu na počítačích s menším výkonem, např. na běžných PC s programem MS Excel. Použití algoritmu v případě navazujícího zpracování za pomocí nelineárních regresních metod je nutností.

obrazová analýza, redukce dat, metoda nejmenších čtverců

The research has been supported by the Grant Agency of the Czech Academy of Sciences under Contract No. IAA201990701.

REFERENCES

BALLESTER, M. A. G., LINGURAU, M. G., AQUIRRE, M. R. and AYACHE, N., 2005: On the adequacy of principal factor analysis for the study of shape variability. Proceedings of Medical Imaging 2005: Image Processing, San Diego, CA, USA, 17 February 2005, pp. 1392

BARTOŇ, S., 2000: Quick algorithms for calculation of coefficients of non-linear and partially continuous functions using the Least Square Method, solution in Maple 6. Proceedings of 8th International Research Conference CO-MAT-TECH 2000, Trnava, October 2000. STU Bratislava, pp. 79–85. ISBN 80–227–1413–5.

BARTOŇ, S., 2007: Stanovení tvaru zemědělské plodiny. Proceedings of 6. Matematický workshop. Brno: FAST VUT Brno, November 2007, pp. 1–12. ISBN 80–214–2741–8.

BARTOŇ, S., 2008: Three dimensional modelling of the peach in Maple. In: CHLEBOUN, J. Programs and Algorithms of numerical Mathematics. 1st ed. Praha. Matematický ústav AV ČR, 2008, pp. 7–14. ISBN 978–80–85823–55–4.

COSTA, L. F. and CESAR, R. M., 2009: Shape Classification and Analysis Theory and Practice. Published by CRC Press, 2009, ISBN 978–0–8493–7929–1.

HAVLÍČEK, M., NEDOMOVÁ, Š., SIMEONOVOVÁ, J., SEVERA, L. and KŘIVÁNEK, I., 2008: On the evaluation of chicken egg shape variability. Acta Universitatis agriculture et silviculture Mendelianae Brunensis 56(5), 69–74.

IGLESIAS, J. E., BRUIJNE, M., LOOG, M., LAUZE, F. and NIELSEN, M., 2007: A Family of Principal Component Analyses for Dealing with Outliers. Proceedings of 10th MICCAI International Conference, October 29 – November 2, Brisbane, Australia, pp. 178–185. ISBN 978-3-540-75758-0

JOLLIFFE, I., 1986: Principal component analysis. Springer, New York, 1986

KLOTZ, B., PYLE D. L. and MACKEY, M., 2007: New Mathematical Modeling Approach for Predicting Microbial Inactivation by High Hydrostatic Pressure. Applied and Environmental Microbiology 73(8), 2468–2478.

LI, T., THONDYKE, B., SCHREIBMANN, E., YANG, Y. and XING, L., 2006: Model-based image reconstruction for four-dimensional PET. Med. Phys. 33(5), 1288–1298.

SEVERA, L., 2007: Response analysis of the dynamic excitation of hen eggs. Acta Universitatis agriculture et silviculture Mendelianae Brunensis 55(5), 137–146.

SEVERA, L., 2008: Development of the peach firmness during harvest period. Acta Universitatis agriculture et silviculture Mendelianae Brunensis 56(4), 169–176.

SÖHN, M., BIRKNER, M., YAN, D. and ALBER, M., 2005: Modelling individual geometric variation based on dominant eigenmodes of organ deformation: implementation and evaluation. Phys. Med. Biol. 50, 5893–5908.

TOMÁNKOVÁ, K., JEŘÁBKOVÁ, P., ZMEŠKAL, O., VESELÁ, M. and HADERKA, J., 2006: Use of Image Analysis to Study Growth and Division of Yeast Cells. Journal of Imaging Science and Technology 50(6), 583–587.

VIDAL, R., MA, Y. and SASTRY, S., 2005: Generalized Principal Component Analysis (GPCA). IEEE Transactions on Pattern Analysis and Machine Inteligence 27(12), 1–15.

WANG, M., PERERA, A. and GUTIERREZ-OSUNA, R., 2004: Principal Discriminants Analysis for small-sample-size problems: Application to chemical sensing. Proceedings of IEEE Sensors 2, 591–594.

YAHYA, A., ZOHADIE, M., KHEIRALLA, A. F., GIEW, S. K. and BOON, N. E., 2009: Mapping system for tractor-implement performance. Computers and Electronics in Agriculture 69, 2–11.

ZADRAVEC, M. AND ŽALIK, B., 2009: A geometric and topological system for supporting agricultural subsidies in Slovenia. Computers and Electronics in Agriculture 69, 92–92.

ZAGRODSKY, V., WALIMBE, V., CASTRO–PAREJA, C. R., JIAN, X. Q., JONG–MIN, S., SHEKHAR, R., 2005: Registration–assisted segmentation of real-time 3–D echocardiographic data using deformable models. IEEE Transactions on Medical Imaging 24 (9), 1089–1099.

ZHONG, D., NOVAIS, J., GRIFT, T. E., BOHN, M. and HAN, J., 2009: Maize root complexity analysis using a Support Vector Machine method. Computers and Electronics in Agriculture 69, 46–50.

Address

doc. RNDr. Stanislav Bartoň, CSc., doc. Ing. Libor Severa, Ph.D., prof. Ing. Jaroslav Buchar, DrSc., Ústav techniky a automobilové dopravy, Mendelova zemědělská a lesnická univerzita v Brně, Zemědělská 1, 613 00 Brno, Česká republika, e-mail: barton@mendelu.cz